

Localization of Brain Activity from EEG/MEG Using MV-PURE Framework

Tomasz Piotrowski^{*,1,2} and Jan Nikadon^{1,2}

¹ Faculty of Physics, Astronomy and Informatics,
Nicolaus Copernicus University, Grudziadzka 5/7, 87-100 Torun, Poland

² Interdisciplinary Center for Modern Technologies,
Nicolaus Copernicus University, Wilenska 4, 87-100 Torun, Poland

Abstract—We consider the problem of localization of sources of brain electrical activity from electroencephalographic (EEG) and magnetoencephalographic (MEG) measurements using spatial filtering techniques. We propose novel reduced-rank activity indices based on the *minimum-variance pseudo-unbiased reduced-rank estimation (MV-PURE)* framework. The main results of this paper establish the key unbiasedness property of the proposed indices and their higher spatial resolution compared with full-rank indices in challenging task of localizing closely positioned and possibly highly correlated sources, especially in low signal-to-noise regime. A numerical example is provided to illustrate the practical applicability of the proposed activity indices. Simulations presented in this paper use open-source EEG/MEG spatial filtering framework freely available at <https://github.com/IS-UMK/supFunSim.git>.

EDICS Category: BIO-SENS, SAM-BEAM, SSP-APPL

*Corresponding author.

I. INTRODUCTION

Electroencephalography (EEG) and magnetoencephalography (MEG) enable measuring electromagnetic fields generated by synchronous post-synaptic electric currents in populations of neurons, using an array of sensors positioned outside the brain [11], [19]. Adaptive spatial filters (beamformers) have been used in array signal processing since the seminal paper by Frost [7]. In EEG and MEG, beamforming has been used for source localization and reconstruction of electrical activity of sources (see [1], [9] for a review). The dominant approach to these problems is to use solutions based on the linearly constrained minimum-variance (LCMV) beamformer [5], [10], [17], [31], [32], [37]. The LCMV beamformer is implemented in virtually all software enabling EEG/MEG source analysis [8], [20], [35] and continues to find research use in EEG/MEG community, see, e.g., [15], [33].

In this paper we focus on source localization from EEG/MEG measurements. The beamformer-based approach to this problem is based on the pioneering idea of an activity index (localizer function) named *neural activity index (NAI)* introduced in [37]. The NAI is a function of source location and is defined as a certain power ratio of the output of the LCMV filter. Its main assumption is that its maxima coincide with locations of active sources. Indeed, several other activity indices based on LCMV beamformer have been introduced since [37], see, for example, [2], [27], [28]. However, neither

NAI, nor the newer activity indices, have been proved to be spatially unbiased, i.e., that they achieve their global maxima if evaluated at locations of sources responsible for observed data. In other words, their main assumption relies in each case on a certain heuristic approach. Only recently, Moiseev et al. [17] has introduced unbiased activity indices (localizers) based on LCMV beamformer. Remarkably, the activity indices introduced in [17] are theoretically unbiased for any signal-to-noise ratio and any level of correlation of activity of sources. Yet, in practice, these factors strongly affect spatial resolution of activity indices.¹ Moreover, it has been demonstrated in [5], [31], [32], [37] and references therein that the LCMV-based solutions may perform sufficiently well only if certain conditions are satisfied by the EEG/MEG forward model, such as uncorrelatedness of the sources, high signal-to-noise ratio (SNR), sufficiently large spatial separation of sources, or the amount of regularization. Thus, it would be desirable to derive activity indices which do not inherit the drawbacks of the LCMV beamformer and offer possibly higher spatial resolution in well-defined settings.

In this paper we introduce activity indices built on the minimum-variance pseudo-unbiased reduced-rank (MV-PURE) estimation framework [21], [25], [26], [39]. We prove that these indices are also unbiased and show that they provide higher spatial resolution in ill-conditioned settings, in which sources can be closely positioned and exhibit correlated activity overwhelmed by noise. Such circumstances arise in neurophysiological research whenever activity of small cortex patch needs to be analysed in detail, e.g., tonotopy in auditory cortex, retinotopy in visual cortex, etc.

The proposed activity indices are natural generalizations of activity indices proposed in [17], just as the MV-PURE framework generalizes linearly-constrained minimum-variance approach to the reduced-rank case. Moreover, both the activity indices proposed in this paper and in [17] are multi-source, meaning that they are functions of combinations of sources' positions. This fact renders an exhaustive search for sources over the entire brain volume infeasible, as the number of possible combinations grows exponentially with the number of sources considered simultaneously active. Thus, for the proposed activity indices we employed the sequential search procedure introduced in [17] which allows finding the sources

¹Spatial resolution is defined in Definition 2 in Section II.

with reasonable computational effort at each iteration.

The paper is organized as follows. In Section II we introduce the notation used in the paper, the EEG/MEG forward model considered, and the definitions of an unbiased activity index and its spatial resolution. We also provide definitions of full-rank activity indices introduced in [17] along with their biased generalizations proposed in [18]. In Section III we propose novel reduced-rank activity indices, prove that they are unbiased, and discuss their spatial resolution as a function of their rank. Section IV provides numerical simulations using open-source EEG/MEG spatial filtering framework available for download at <https://github.com/IS-UMK/supFunSim.git>.

A short preliminary versions of the paper were presented at conferences [22], [23].

II. PRELIMINARIES

A. Notation

Assume \mathbf{x} to be a vector of real-valued random variables x_1, \dots, x_k , each with a finite variance. The expected value of \mathbf{x} is denoted by $\mathbb{E}[\mathbf{x}]$ and the covariance matrix of \mathbf{x} is denoted by $\mathcal{D}[\mathbf{x}]$. \mathbf{I}_l stands for identity matrix of size l , while \mathbf{I}_r^l stands for a diagonal matrix of size l in which the first r entries at the main diagonal are equal to 1 and all other entries are equal to 0. By $[\mathbf{A}]_{i,j}$ we denote the $i \times j$ principal submatrix of a matrix \mathbf{A} . We call \mathbf{A} ill-conditioned if some of its singular values are close to zero. By $\text{tr}\{\mathbf{A}\}$ we denote the trace of a square matrix \mathbf{A} . Let \mathbf{A} be similar to a symmetric matrix, i.e., $\mathbf{A} = \mathbf{P}^{-1}\mathbf{S}\mathbf{P}$, where \mathbf{P} is invertible and \mathbf{S} symmetric. Then, $\lambda(\mathbf{A})$ denotes the vector of eigenvalues of \mathbf{A} organized in non-increasing order. We assume that all eigenvalue decompositions considered have eigenvalues organized in non-increasing order. Let \mathbf{A} and \mathbf{B} be symmetric matrices. Then, relation $\mathbf{A} \succeq \mathbf{B}$ denotes Loewner ordering, i.e., $\mathbf{A} - \mathbf{B}$ is positive semidefinite [14]. Finally, for a given positive (semi)definite matrix \mathbf{A} , we denote by $\mathbf{A}^{1/2}$ the unique matrix such that $\mathbf{A}^{1/2}\mathbf{A}^{1/2} = \mathbf{A}$ and $\mathbf{A}^{1/2}$ is also positive (semi)definite [14].

The position of a single dipole source is a triple of Cartesian coordinates θ . We denote by $\boldsymbol{\theta} = (\theta_1, \dots, \theta_l)$ an l -tuple of Cartesian coordinates of l sources, where θ_i denotes the position of the i -th source, $i = 1, \dots, l$. The leadfield matrix establishing electromagnetic field propagation model between l dipole sources and m sensors is defined as $\mathbf{H}(\boldsymbol{\theta}) = (h(\theta_1), \dots, h(\theta_l)) \in \mathbb{R}^{m \times l}$, where $h(\theta_i) \in \mathbb{R}^m$ is the leadfield vector of the i -th source for $i = 1, \dots, l$. The set of columns of $\mathbf{H}(\boldsymbol{\theta})$ is denoted by $\{\mathbf{H}(\boldsymbol{\theta})\}$. The positions of the l_0 sources active during the measurement are denoted by $\boldsymbol{\theta}_0 = (\theta_{0,1}, \dots, \theta_{0,l_0})$. To simplify notation, explicit dependence on $\boldsymbol{\theta}$ is omitted whenever possible and values evaluated at $\boldsymbol{\theta}_0$ are denoted by adding the 0 subscript, e.g., the leadfield matrix evaluated at $\boldsymbol{\theta}_0$ is denoted by $\mathbf{H}_0 := \mathbf{H}(\boldsymbol{\theta}_0)$.

B. EEG/MEG Forward Model

We consider l_0 dipole sources of brain electrical activity and EEG/MEG measurements obtained with $m > l_0$ sensors. We assume that the sources' positions $\boldsymbol{\theta}_0$ are fixed during the measurement period. Then, the $m \times 1$ random vector \mathbf{y}

composed of the measurements at a given time instant can be modeled as [19], [37]:

$$\mathbf{y} = \mathbf{H}_0\mathbf{q}_0 + \mathbf{n}, \quad (1)$$

where $\mathbf{H}_0 := \mathbf{H}(\boldsymbol{\theta}_0) \in \mathbb{R}^{m \times l_0}$ is the array response (leadfield) matrix corresponding to sources at locations $\boldsymbol{\theta}_0$, $\mathbf{q}_0 \in \mathbb{R}^{l_0}$ is a random vector representing electric/magnetic dipole moments at $\boldsymbol{\theta}_0$, and random vector $\mathbf{n} \in \mathbb{R}^m$ expresses background activity along with noise measured at the sensors.

We assume that the leadfield matrix $\mathbf{H}(\boldsymbol{\theta})$ has full column rank for any set of sources $\boldsymbol{\theta}$ [31]. We also assume that \mathbf{q}_0 and \mathbf{n} are zero-mean weakly stationary stochastic processes, covariance matrices $\mathcal{D}[\mathbf{q}_0] := \mathbf{Q}$ and $\mathcal{D}[\mathbf{n}] := \mathbf{N}$ are positive definite, and that \mathbf{q}_0 and \mathbf{n} are uncorrelated. This implies in particular that the covariance matrix of observed signal is also positive definite and is of the form

$$\mathcal{D}[\mathbf{y}] := \mathbf{R} = \mathbf{H}_0\mathbf{Q}\mathbf{H}_0^t + \mathbf{N}.$$

C. Key Properties of Activity Indices

Definition 1. Define by $\{\mathbf{H}(\boldsymbol{\theta})\}$ the set of columns (leadfields) of a leadfield matrix $\mathbf{H}(\boldsymbol{\theta}) \in \mathbb{R}^{m \times l}$ of l sources. We call a function $f : \{\mathbf{H}(\boldsymbol{\theta})\} \rightarrow \mathbb{R}_+$ an activity index. We say that an activity index f is unbiased if [17], [31]

$$\{\mathbf{H}(\boldsymbol{\theta}_0)\} \in \left\{ \arg \max_{\{\mathbf{H}(\boldsymbol{\theta})\}} f(\{\mathbf{H}(\boldsymbol{\theta})\}) \right\}. \quad (2)$$

A few remarks on Definition 1 are in place here.

- An argument of an activity index f is the set of leadfields $\{\mathbf{H}(\boldsymbol{\theta})\}$ of arbitrary number of sources l .
- In the above definition, a leadfield $h(\theta) \in \mathbb{R}^m$ serves as a unique identifier of a source at θ . This is justified by the linear independence of columns of a leadfield matrix $\mathbf{H}(\boldsymbol{\theta})$ for any set of sources $\boldsymbol{\theta}$ [31]. Thus, we may simplify below the notation of an activity index and represent its argument by $\boldsymbol{\theta}$ in place of $\{\mathbf{H}(\boldsymbol{\theta})\}$.
- It should be also noted that $\boldsymbol{\theta}_0$ maximizes an unbiased activity index without any assumptions on \mathbf{Q} and \mathbf{N} , and in particular, without any assumptions on the signal-to-noise ratio.
- Finally, we note that the set of maximizers of an unbiased activity index may contain elements other than $\boldsymbol{\theta}_0$, as the inverse problem in EEG/MEG is inherently ill-posed [12].

Definition 2. Consider two unbiased activity indices f_1 and f_2 . We say that f_1 has higher spatial resolution than f_2 if [17], [31]

$$\forall \boldsymbol{\theta} \ f_1(\boldsymbol{\theta}) \leq f_2(\boldsymbol{\theta}) \quad \text{and} \quad f_1(\boldsymbol{\theta}_0) = f_2(\boldsymbol{\theta}_0). \quad (3)$$

D. MAI and MPZ Unbiased Activity Indices

The work [17] introduced, among others, two unbiased activity indices which extend to the multi-source case previously known single-source indices maximizing certain signal-to-noise ratios at the output of the *linearly constrained minimum-variance (LCMV)* filter [7], [31], [37] (see Appendix A for the optimization problem leading to the LCMV filter):

$$\mathbf{W}(\boldsymbol{\theta}) = \mathbf{S}(\boldsymbol{\theta})^{-1}\mathbf{H}(\boldsymbol{\theta})^t\mathbf{R}^{-1}, \quad (4)$$

where $\mathbf{S}(\boldsymbol{\theta}) \in \mathbb{R}^{l \times l}$ is a positive definite matrix of the form

$$\mathbf{S} := \mathbf{S}(\boldsymbol{\theta}) = \mathbf{H}(\boldsymbol{\theta})^t \mathbf{R}^{-1} \mathbf{H}(\boldsymbol{\theta}) := \mathbf{H}^t \mathbf{R}^{-1} \mathbf{H} \succ 0. \quad (5)$$

The signal-to-noise ratios of interest are obtained as follows: the covariance matrix of the signal $\hat{\mathbf{q}}_0 = \mathbf{W}(\boldsymbol{\theta})\mathbf{y}$ reconstructed using LCMV filter is

$$\mathcal{D}[\mathbf{W}(\boldsymbol{\theta})\mathbf{y}] = \mathbf{W}(\boldsymbol{\theta})\mathbf{R}\mathbf{W}(\boldsymbol{\theta})^t = \mathbf{S}^{-1}. \quad (6)$$

Assume now that only background activity along with noise (i.e., \mathbf{n} in (1)) is observed. Then, \mathbf{R} reduces to \mathbf{N} , and the LCMV filter becomes

$$\mathbf{W}_N(\boldsymbol{\theta}) = \mathbf{G}(\boldsymbol{\theta})^{-1} \mathbf{H}(\boldsymbol{\theta})^t \mathbf{N}^{-1}, \quad (7)$$

where $\mathbf{G}(\boldsymbol{\theta}) \in \mathbb{R}^{l \times l}$ is a positive definite matrix of the form

$$\mathbf{G} := \mathbf{G}(\boldsymbol{\theta}) = \mathbf{H}(\boldsymbol{\theta})^t \mathbf{N}^{-1} \mathbf{H}(\boldsymbol{\theta}) := \mathbf{H}^t \mathbf{N}^{-1} \mathbf{H} \succ 0. \quad (8)$$

Then, one has in such a case that

$$\mathcal{D}[\mathbf{W}_N(\boldsymbol{\theta})\mathbf{n}] = \mathbf{W}_N(\boldsymbol{\theta})\mathbf{N}\mathbf{W}_N(\boldsymbol{\theta})^t = \mathbf{G}^{-1}. \quad (9)$$

For a single source case of $l = 1$, \mathbf{S} and \mathbf{G} become scalar values and the ratio

$$\mathcal{D}[\mathbf{W}(\boldsymbol{\theta})\mathbf{y}]/\mathcal{D}[\mathbf{W}_N(\boldsymbol{\theta})\mathbf{n}] - 1 = \mathbf{S}^{-1}/\mathbf{G}^{-1} - 1 = \mathbf{G}\mathbf{S}^{-1} - 1 \quad (10)$$

has been known in literature as *neural activity index* since its introduction in the seminal paper [37].²

Moreover, assuming full signal \mathbf{y} in model (1) is observed, the covariance matrix of the noise projected by the LCMV filter is of the form:

$$\begin{aligned} \mathcal{D}[\mathbf{W}(\boldsymbol{\theta})\mathbf{n}] = \\ \mathbf{S}^{-1} \mathbf{H}(\boldsymbol{\theta})^t \mathbf{R}^{-1} \mathbf{N} \mathbf{R}^{-1} \mathbf{H}(\boldsymbol{\theta}) \mathbf{S}^{-1} = \mathbf{S}^{-1} \mathbf{T} \mathbf{S}^{-1}, \end{aligned} \quad (11)$$

where $\mathbf{T} \in \mathbb{R}^{l \times l}$ is a positive definite matrix such that

$$\begin{aligned} \mathbf{T} := \mathbf{T}(\boldsymbol{\theta}) = \mathbf{H}(\boldsymbol{\theta})^t \mathbf{R}^{-1} \mathbf{N} \mathbf{R}^{-1} \mathbf{H}(\boldsymbol{\theta}) := \\ \mathbf{H}^t \mathbf{R}^{-1} \mathbf{N} \mathbf{R}^{-1} \mathbf{H} \succ 0. \end{aligned} \quad (12)$$

Then, for a single source case of $l = 1$, the ratio

$$\begin{aligned} \mathcal{D}[\mathbf{W}(\boldsymbol{\theta})\mathbf{y}]/\mathcal{D}[\mathbf{W}(\boldsymbol{\theta})\mathbf{n}] - 1 = \\ \mathbf{S}^{-1}/(\mathbf{S}^{-1} \mathbf{T} \mathbf{S}^{-1}) - 1 = \mathbf{S} \mathbf{T}^{-1} - 1, \end{aligned} \quad (13)$$

has been known in literature as *pseudo-Z index* [29].

The work [17] extended single-source activity indices in (10) and (13) by introducing, respectively:

- *Multi-source Activity Index (MAI)* defined in [17] as

$$MAI(\boldsymbol{\theta}) = \text{tr}\{\mathbf{G}\mathbf{S}^{-1}\} - l, \quad (14)$$

- *Multi-source Pseudo-Z index (MPZ)* defined in [17] as

$$MPZ(\boldsymbol{\theta}) = \text{tr}\{\mathbf{S}\mathbf{T}^{-1}\} - l. \quad (15)$$

It has been proved in [17] that *MAI* and *MPZ* activity indices are unbiased in the sense of Definition 1. Moreover, it has been also proved there that these localizers satisfy the

saturation property: an increase of the number of sources l above l_0 results in the same maximizing values of *MAI* and *MPZ* activity indices as those obtained for l_0 . Moreover, the maximizing values of *MAI* and *MPZ* activity indices obtained for l such that $1 \leq l \leq l_0$ are monotonically increasing with increasing l until l_0 is reached.

Remark 1. *The above facts suggest a way to determine the number of sources l_0 [17]: iterate with respect to l starting with $l = 1$, and compute maximum value of *MAI* or *MPZ* until plateau is reached. Thus, we assume below that l is such that $1 \leq l \leq l_0$ and that the true number of sources l_0 is known.*

It has been also established in [17] that *MPZ* has higher spatial resolution than *MAI*. See Appendix B for a sketch of proof of this fact.

E. Extensions of *MAI* and *MPZ* Activity Indices

An interesting extension of results in [17] is provided in [18], where it has been proved that all combinations of eigenvalues of $\mathbf{G}\mathbf{S}^{-1}$ and all combinations of eigenvalues of $\mathbf{S}\mathbf{T}^{-1}$ have stationary points at $\boldsymbol{\theta}_0$, extending in this sense *MAI* and *MPZ* localizers. Moreover, Monte-Carlo simulations presented in [18] showed that the sum of the largest eigenvalues yielded the most stable results.

Let $r \in \mathbb{N}$ be a natural number less than l_0 . Following [18], we consider the extensions of *MAI* and *MPZ* activity indices defined as

$$MAI_{ext}(\boldsymbol{\theta}, r) = \sum_{i=1}^r \lambda_i(\mathbf{G}\mathbf{S}^{-1}) - r, \quad 1 \leq r \leq l_0, \quad (16)$$

and

$$MPZ_{ext}(\boldsymbol{\theta}, r) = \sum_{i=1}^r \lambda_i(\mathbf{S}\mathbf{T}^{-1}) - r, \quad 1 \leq r \leq l_0, \quad (17)$$

respectively.

We note that *MAI_{ext}* and *MPZ_{ext}* activity indices are not unbiased in the sense of Definition 1. However, due to the fact that all combinations of eigenvalues of $\mathbf{G}\mathbf{S}^{-1}$ and all combinations of eigenvalues of $\mathbf{S}\mathbf{T}^{-1}$ have stationary points at $\boldsymbol{\theta}_0$, the *MAI_{ext}* and *MPZ_{ext}* activity indices are called *unbiased in a broad sense* in [18].

We also note that if *MAI_{ext}* and *MPZ_{ext}* activity indices are evaluated for r such that $r > l$, we naturally assume that $r = l$ is selected.

III. PROPOSED ACTIVITY INDICES

The *MAI* and *MPZ* localizers introduced in Section II-D are based on the LCMV filter, whose performance is known to be poor if sources are strongly correlated or the forward model is ill-conditioned as a result of large condition number of leadfield matrix and/or high background activity and measurement noise, see, e.g., [26], [37] and references therein. It is therefore intriguing to find how these drawbacks of the LCMV filter affect unbiased *MAI* and *MPZ* activity indices in terms of their spatial resolution.

²In [37], *neural activity index* was defined without subtracting one from the power ratio $\mathbf{G}\mathbf{S}^{-1}$. We have done so here to emphasize the relation between single-source indices and their multi-source generalizations introduced below.

To this end, we shall consider below the following forward model equivalent to (1):

$$\mathbf{y} = \mathbf{H}_0 \mathbf{Q}^{1/2} \mathbf{Q}^{-1/2} \mathbf{q}_0 + \mathbf{n} = \mathbf{H}'_0 \mathbf{q}'_0 + \mathbf{n}, \quad (18)$$

with $\mathbf{H}'_0 = \mathbf{H}_0 \mathbf{Q}^{1/2}$ and $\mathbf{q}'_0 = \mathbf{Q}^{-1/2} \mathbf{q}_0$ such that $\mathcal{D}[\mathbf{q}'_0] = \mathbf{I}_{l_0}$. Then, letting $\mathbf{H}' := \mathbf{H}([\mathbf{Q}]_{l \times l})^{1/2}$ we may define \mathbf{S}' , \mathbf{G}' , and \mathbf{T}' as above, by using \mathbf{H}' in place of \mathbf{H} , e.g., $\mathbf{S}' := (\mathbf{H}')^t \mathbf{R}^{-1} \mathbf{H}'$.

A. Reduced-Rank Approach

One of the common ways to remedy the drawbacks of the LCMV filter is to apply reduced-rank solutions in situations where the LCMV filter performs poorly [30], [34], [38]. Following this line, in this paper we develop activity indices which are reduced-rank extensions of *MAI* and *MPZ* localizers.

We note first that the LCMV filter designed for model (18) is of the following form:

$$\mathbf{W}'(\boldsymbol{\theta}) := \mathbf{S}'(\boldsymbol{\theta})^{-1} \mathbf{H}'(\boldsymbol{\theta})^t \mathbf{R}^{-1} = \mathbf{Q}^{-1/2} \mathbf{W}(\boldsymbol{\theta}). \quad (19)$$

Let $r \in \mathbb{N}$ be such that $1 \leq r \leq l_0$. Below, we propose activity indices based on the MV-PURE filter [25], given in terms of model (18) as

$$\mathbf{W}'_{RR}(\boldsymbol{\theta}) = \mathbf{P}'_{\mathbf{S}'}(\boldsymbol{\theta}) \mathbf{W}'(\boldsymbol{\theta}), \quad (20)$$

where by $\mathbf{P}'_{\mathbf{S}'}(\boldsymbol{\theta}) = \mathbf{V} \mathbf{I}'_r \mathbf{V}^t$ we denote orthogonal projection matrix onto subspace spanned by eigenvectors corresponding to the r largest eigenvalues of \mathbf{S}' given with eigenvalue decomposition $\mathbf{S}' = \mathbf{V} \boldsymbol{\Lambda} \mathbf{V}^t$. The MV-PURE filter is a natural reduced-rank extension of the LCMV filter, *cf.* optimization problems given in Appendix A, for which $\mathbf{W}'(\boldsymbol{\theta})$ and $\mathbf{W}'_{RR}(\boldsymbol{\theta})$ are solutions.

Consider now the signal-to-noise ratios of the MV-PURE filter. Owing to the symmetry of $\mathbf{P}'_{\mathbf{S}'}(\boldsymbol{\theta})$, the expressions corresponding to (6) and (9) are, respectively,

$$\begin{aligned} \mathcal{D}[\mathbf{W}'_{RR}(\boldsymbol{\theta}) \mathbf{y}] &= \\ \mathbf{P}'_{\mathbf{S}'}(\boldsymbol{\theta}) \mathbf{W}'(\boldsymbol{\theta}) \mathbf{R} (\mathbf{P}'_{\mathbf{S}'}(\boldsymbol{\theta}) \mathbf{W}'(\boldsymbol{\theta}))^t &= \mathbf{P}'_{\mathbf{S}'}(\boldsymbol{\theta}) (\mathbf{S}')^{-1} \mathbf{P}'_{\mathbf{S}'}(\boldsymbol{\theta}), \end{aligned} \quad (21)$$

and

$$\begin{aligned} \mathcal{D}[\mathbf{W}'_{RRN}(\boldsymbol{\theta}) \mathbf{n}] &= \\ \mathbf{P}'_{\mathbf{S}'}(\boldsymbol{\theta}) \mathbf{W}'_N(\boldsymbol{\theta}) \mathbf{N} (\mathbf{P}'_{\mathbf{S}'}(\boldsymbol{\theta}) \mathbf{W}'_N(\boldsymbol{\theta}))^t &= \mathbf{P}'_{\mathbf{S}'}(\boldsymbol{\theta}) (\mathbf{G}')^{-1} \mathbf{P}'_{\mathbf{S}'}(\boldsymbol{\theta}), \end{aligned} \quad (22)$$

where $\mathbf{W}'_{RRN} := \mathbf{P}'_{\mathbf{S}'}(\boldsymbol{\theta}) \mathbf{W}'_N$ with

$$\mathbf{W}'_N(\boldsymbol{\theta}) := \mathbf{G}'(\boldsymbol{\theta}) \mathbf{H}'(\boldsymbol{\theta})^t \mathbf{N}^{-1} = \mathbf{Q}^{-1/2} \mathbf{W}_N(\boldsymbol{\theta}),$$

cf. (19).³ Then, in view of idempotency of $\mathbf{P}'_{\mathbf{S}'}(\boldsymbol{\theta})$, and the fact that

$$\begin{aligned} \mathbf{P}'_{\mathbf{S}'}(\boldsymbol{\theta}) (\mathbf{S}')^{-1} \mathbf{P}'_{\mathbf{S}'}(\boldsymbol{\theta}) &= \mathbf{V} \mathbf{I}'_r \mathbf{V}^t \mathbf{V} \boldsymbol{\Lambda}^{-1} \mathbf{V}^t \mathbf{V} \mathbf{I}'_r \mathbf{V}^t = \\ \mathbf{V} \mathbf{I}'_r \boldsymbol{\Lambda}^{-1} \mathbf{I}'_r \mathbf{V}^t &= \mathbf{V} \boldsymbol{\Lambda}^{-1} \mathbf{I}'_r \mathbf{V}^t = \mathbf{V} \boldsymbol{\Lambda}^{-1} \mathbf{V}^t \mathbf{V} \mathbf{I}'_r \mathbf{V}^t = \\ &= (\mathbf{S}')^{-1} \mathbf{P}'_{\mathbf{S}'}(\boldsymbol{\theta}), \end{aligned} \quad (23)$$

³If only background activity \mathbf{n} is observed, we could also use the alternative form of the filter $\mathbf{W}'_{RRN} := \mathbf{P}'_{\mathbf{G}'}(\boldsymbol{\theta}) \mathbf{W}'_N$. However, this would lead to a more involved form of the proposed index, with both $\mathbf{P}'_{\mathbf{G}'}(\boldsymbol{\theta})$ and $\mathbf{P}'_{\mathbf{S}'}(\boldsymbol{\theta})$ present.

and proceeding analogously as in [17] by generalizing the ratio $\mathcal{D}[\mathbf{W}'_{RR}(\boldsymbol{\theta}) \mathbf{y}] / \mathcal{D}[\mathbf{W}'_{RRN}(\boldsymbol{\theta}) \mathbf{n}]$ to the multi-source case (*cf.* (10)), we obtain the following reduced-rank extension of the *MAI* activity index (14):

$$\begin{aligned} MAI_{RR}(\boldsymbol{\theta}, r) &= \text{tr}\{\mathbf{P}'_{\mathbf{S}'}(\boldsymbol{\theta}) \mathbf{G}' \mathbf{P}'_{\mathbf{S}'}(\boldsymbol{\theta}) \mathbf{P}'_{\mathbf{S}'}(\boldsymbol{\theta}) (\mathbf{S}')^{-1} \mathbf{P}'_{\mathbf{S}'}(\boldsymbol{\theta})\} - r = \\ &= \text{tr}\{\mathbf{G}' \mathbf{P}'_{\mathbf{S}'}(\boldsymbol{\theta}) (\mathbf{S}')^{-1} \mathbf{P}'_{\mathbf{S}'}(\boldsymbol{\theta})\} - r := \\ &= \text{tr}\{\mathbf{G}' (\mathbf{S}')^{-1} \mathbf{P}'_{\mathbf{S}'}(\boldsymbol{\theta})\} - r, \quad 1 \leq r \leq l_0. \end{aligned} \quad (24)$$

Similarly, for the generalization of the *MPZ* activity index to the reduced-rank case, we consider now the expression of the covariance matrix of the noise projected by the MV-PURE filter, *cf.* (11):

$$\begin{aligned} \mathcal{D}[\mathbf{W}'_{RR}(\boldsymbol{\theta}) \mathbf{n}] &= \\ \mathbf{P}'_{\mathbf{S}'}(\boldsymbol{\theta}) (\mathbf{S}')^{-1} \mathbf{H}'(\boldsymbol{\theta})^t \mathbf{R}^{-1} \mathbf{N} \mathbf{R}^{-1} \mathbf{H}'(\boldsymbol{\theta}) (\mathbf{S}')^{-1} \mathbf{P}'_{\mathbf{S}'}(\boldsymbol{\theta}). \end{aligned} \quad (25)$$

Then, from (13), and in view of the above derivation for *MAI*_{RR}, it is clear that the generalized ratio $\mathcal{D}[\mathbf{W}'_{RR}(\boldsymbol{\theta}) \mathbf{y}] / \mathcal{D}[\mathbf{W}'_{RR}(\boldsymbol{\theta}) \mathbf{n}]$ defining *MPZ*_{RR} activity index will be of the form

$$MPZ_{RR}(\boldsymbol{\theta}, r) := \text{tr}\{\mathbf{S}' (\mathbf{T}')^{-1} \mathbf{P}'_{\mathbf{S}'}(\boldsymbol{\theta})\} - r, \quad 1 \leq r \leq l_0. \quad (26)$$

We note that, similarly as for *MAI*_{ext} and *MPZ*_{ext} localizers introduced in Section II-E, we assume that if *MAI*_{RR} or *MPZ*_{RR} localizers are evaluated for r such that $r > l$, we assume that $r = l$ is selected.

B. Key Properties of *MAI*_{RR} and *MPZ*_{RR} Activity Indices

We begin this section with the following lemma.

Lemma 1. *Let r be a natural number less than l_0 . Then*

$$MAI_{RR}(\boldsymbol{\theta}, r) \leq \sum_{i=1}^r \lambda_i(\mathbf{R} \mathbf{N}^{-1}) - r = \sum_{i=1}^r \lambda_i(\mathbf{G}'_0). \quad (27)$$

Proof: See Appendix C.

We are now ready to prove the following theorem.

Theorem 1. *Let r be a natural number less than l_0 . Then, *MAI*_{RR} and *MPZ*_{RR} activity indices are unbiased. Moreover, *MPZ*_{RR} has higher spatial resolution than *MAI*_{RR} for the same rank constraint r . In particular, one has*

$$MAI_{RR}(\boldsymbol{\theta}_0, r) = MPZ_{RR}(\boldsymbol{\theta}_0, r) = \sum_{i=1}^r \lambda_i(\mathbf{G}'_0). \quad (28)$$

Proof: See Appendix D.

Theorem 1 introduces two families of unbiased activity indices parameterized by rank. The important questions are: when it is useful to lower the rank of a given unbiased activity index, and how this parameter should be selected in practice. To provide insight into these questions, we begin with the following propositions.

Proposition 1. *Let r be a natural number less than l_0 . Then*

$$\begin{aligned} MAI(\boldsymbol{\theta}_0) - MAI_{RR}(\boldsymbol{\theta}_0, r) &= \\ MPZ(\boldsymbol{\theta}_0) - MPZ_{RR}(\boldsymbol{\theta}_0, r) &= \sum_{i=r+1}^{l_0} \lambda_i(\mathbf{G}'_0). \end{aligned} \quad (29)$$

Proof: The proof is obtained immediately from (28) in Theorem 1. ■

Proposition 2. *Let r be a natural number less than l_0 . Then*

$$\begin{aligned} MAI_{RR}(\boldsymbol{\theta}, r) &\leq MAI_{RR}(\boldsymbol{\theta}, r+1) \leq \dots \\ &\leq MAI_{RR}(\boldsymbol{\theta}; l_0) = MAI(\boldsymbol{\theta}), \end{aligned} \quad (30)$$

and similarly

$$\begin{aligned} MPZ_{RR}(\boldsymbol{\theta}, r) &\leq MPZ_{RR}(\boldsymbol{\theta}, r+1) \leq \dots \\ &\leq MPZ_{RR}(\boldsymbol{\theta}; l_0) = MPZ(\boldsymbol{\theta}). \end{aligned} \quad (31)$$

Proof: See Appendix E.

From (29), it is seen in particular that if the trailing eigenvalues $\lambda_{r+1}(\mathbf{G}'_0), \dots, \lambda_{l_0}(\mathbf{G}'_0)$ of \mathbf{G}'_0 are close to zero for some $r < l_0$, the maximizing value will be almost identical for activity indices of ranks r, \dots, l_0 . Then, taking into account Definition 2, we conclude from (30) and (31) that in such a case, the activity index of rank r provides approximately the highest spatial resolution among activity indices of ranks r, \dots, l_0 . Fig. 1 below illustrates such situation.

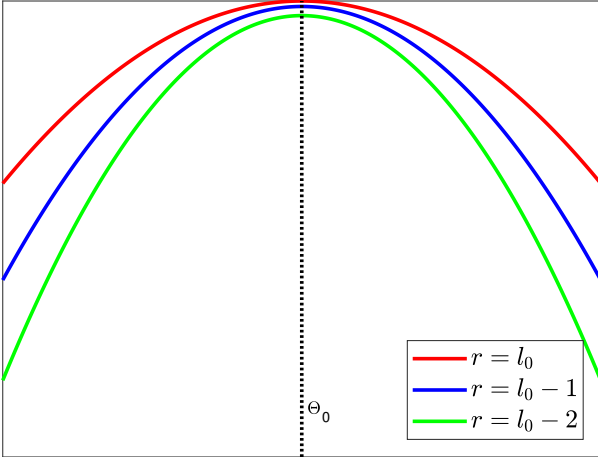


Fig. 1: Theoretical graphs of $MAI_{RR}(\boldsymbol{\theta}, r)$ and $MPZ_{RR}(\boldsymbol{\theta}, r)$ for $r \in \{l_0 - 2, l_0 - 1, l_0\}$. In the situation depicted in this figure, the trailing eigenvalues $\lambda_{l_0-1}(\mathbf{G}'_0)$ and $\lambda_{l_0}(\mathbf{G}'_0)$ of \mathbf{G}'_0 are close to zero, resulting in approximately the same maximum value at $\boldsymbol{\theta}_0$ of $MAI_{RR}(\boldsymbol{\theta}, r)$ and $MPZ_{RR}(\boldsymbol{\theta}, r)$ for $r \in \{l_0 - 2, l_0 - 1, l_0\}$, cf. (29).

In view of the above analysis, we should find now when the trailing eigenvalues $\lambda_{r+1}(\mathbf{G}'_0), \dots, \lambda_{l_0}(\mathbf{G}'_0)$ of \mathbf{G}'_0 are close to zero for some $r < l_0$. To this end, we note first that

$$\begin{aligned} \lambda_i(\mathbf{G}'_0) &= \lambda_i(\mathbf{Q}^{1/2} \mathbf{H}_0^t \mathbf{N}^{-1} \mathbf{H}_0 \mathbf{Q}^{1/2}) = \\ &= \lambda_i(\mathbf{Q} \mathbf{H}_0^t \mathbf{N}^{-1} \mathbf{H}_0) = \lambda_i(\mathbf{H}_0^t \mathbf{N}^{-1} \mathbf{H}_0 \mathbf{Q}), \quad 1 \leq i \leq l_0. \end{aligned} \quad (32)$$

Then, from Fact 4 in Appendix G we obtain, upon setting $k = 1$ therein, that for $i \in \{1, \dots, l_0\}$ one has

$$\lambda_i(\mathbf{G}'_0) \leq \lambda_i(\mathbf{Q}) \lambda_1(\mathbf{H}_0^t \mathbf{N}^{-1} \mathbf{H}_0), \quad (33)$$

and similarly

$$\lambda_i(\mathbf{G}'_0) \leq \lambda_1(\mathbf{Q}) \lambda_i(\mathbf{H}_0^t \mathbf{N}^{-1} \mathbf{H}_0). \quad (34)$$

It is seen, therefore, that $\sum_{i=r+1}^{l_0} \lambda_i(\mathbf{G}'_0)$ in (29) will be close to 0 for some $r < l_0$, provided $\lambda_{r+1}(\mathbf{Q}), \dots, \lambda_{l_0}(\mathbf{Q})$ or $\lambda_{r+1}(\mathbf{H}_0^t \mathbf{N}^{-1} \mathbf{H}_0), \dots, \lambda_{l_0}(\mathbf{H}_0^t \mathbf{N}^{-1} \mathbf{H}_0)$ are close to zero. The former occurs if the activity is heavily correlated among some sources, and the latter if the leadfield matrix \mathbf{H}_0 is ill-conditioned, and especially if the eigenvalues of \mathbf{N} are large, implying low signal-to-noise ratio. From our experience with EEG/MEG forward models, \mathbf{H}_0 is likely to be ill-conditioned if some of the active sources are closely positioned.

The remaining question is how the eigenvalues of \mathbf{G}'_0 in (32) can be estimated in practice, as neither \mathbf{Q} nor \mathbf{H}_0 are observable. However, we note that

$$\begin{aligned} \lambda_i(\mathbf{R} \mathbf{N}^{-1}) &= \lambda_i((\mathbf{H}_0 \mathbf{Q} \mathbf{H}_0^t + \mathbf{N}) \mathbf{N}^{-1}) = \\ &= \lambda_i(\mathbf{H}_0 \mathbf{Q} \mathbf{H}_0^t \mathbf{N}^{-1} + \mathbf{I}_m) = \lambda_i(\mathbf{Q} \mathbf{H}_0^t \mathbf{N}^{-1} \mathbf{H}_0) + 1 = \\ &= \lambda_i(\mathbf{G}'_0) + 1, \quad 1 \leq i \leq l_0. \end{aligned} \quad (35)$$

The covariance matrices \mathbf{R} and \mathbf{N} can be estimated from the available measurements, with the latter obtainable from pre-stimulus interval of the experiment or directly from the estimated spectrum of \mathbf{R} if white noise is assumed [31].

We close this section with a proposition showing that the proposed activity indices would have higher spatial resolution, for the same rank constraint r , than the extensions of MAI and MPZ activity indices of the forms (16) and (17), even if the latter were unbiased.

Proposition 3. *Let r be a natural number less than l_0 , and consider MAI_{ext} and MPZ_{ext} localizers of the forms (16) and (17), respectively. Then*

$$MAI_{RR}(\boldsymbol{\theta}, r) \leq MAI_{ext}(\boldsymbol{\theta}, r), \quad (36)$$

and

$$MPZ_{RR}(\boldsymbol{\theta}, r) \leq MPZ_{ext}(\boldsymbol{\theta}, r). \quad (37)$$

Moreover,

$$\begin{aligned} MAI_{RR}(\boldsymbol{\theta}_0, r) &= MPZ_{RR}(\boldsymbol{\theta}_0, r) = \\ &= MAI_{ext}(\boldsymbol{\theta}_0, r) = MPZ_{ext}(\boldsymbol{\theta}_0, r) = \sum_{i=1}^r \lambda_i(\mathbf{G}'_0). \end{aligned} \quad (38)$$

Proof: See Appendix F.

IV. ITERATIVE IMPLEMENTATION AND SIMULATIONS

A. Iterative Implementation

In view of our assumption introduced in Remark 1, the number of active sources l_0 is known. Thus, it may seem at first that it is sufficient to evaluate multi-source indices for $l = l_0$ only. However, brute-force evaluation of a multi-source index over l_0 -dimensional domain is infeasible, as it contains $\binom{s}{l_0}$ elements, where s is the total number of all possible locations of active sources.

Therefore, for the numerical implementation of the proposed indices, we follow [17] and adapt the iterative procedure used previously for MAI and MPZ activity indices.⁴ This procedure

⁴The iterative procedure used in [17] considers also finding orientation of the dipole sources. We have omitted this step in the proposed implementation, as in this paper we focus on the source localization problem.

discovers locations of sources sequentially, beginning with the strongest source. As described in [17], such approach meets the specifics of the inverse problem in EEG/MEG well, and is capable of closely approximating the optimal solution. The algorithm works as follows:

Algorithm 1 Iterative discovery of sources using multi-source activity index

Input: parameters l_0, s, r , activity index $f(\theta, r)$ in

```

  Initialisation
1:  $\theta_0 = \{\emptyset\}$ 
  LOOP Process
2: for  $l = 1$  to  $l_0$  do
3:   for  $i = 1$  to  $s$  do
4:     set  $\theta_i = \theta_0 \cup \{\theta_i\}$ 
5:   end for
6:   if  $l \leq r$  then
7:      $\theta_0 = \arg \max_{\theta_1, \dots, \theta_s} f(\theta_i, l)$ 
8:   else
9:      $\theta_0 = \arg \max_{\theta_1, \dots, \theta_s} f(\theta_i, r)$ 
10:  end if
11: end for
12: return  $\theta_0$ 

```

We observe that the iterative process described in Algorithm 1 produces for $l \leq r$ exactly the same output as its version used in [17], since for these iterations the activity indices of (full) rank l are used. However, for $l > r$, the reduced-rank approach is used in the above implementation, and thus is aimed at finding weaker sources at later iterations. In such a case, one would need to estimate $[\mathbf{Q}]_{l \times l}$ for \mathbf{H}' needed for MAI_{RR} and MPZ_{RR} localizers, cf. (18), (24) and (26). However, for the iterative procedure considered here, this is hardly achievable, as the estimate of $[\mathbf{Q}]_{l \times l}$ would necessarily depend on sources found in previous iterations, some of which may be localized with an error. This in turn prohibits accurate estimation of $[\mathbf{Q}]_{l \times l}$, and consequently seriously limits localization accuracy in subsequent iterations. To circumvent this difficulty, we assume below that for iterations $l > r$ the activity of sources is uncorrelated, which frees us from the need of computing the estimate of $[\mathbf{Q}]_{l \times l}$ at these iterations.

We note that Algorithm 1 requires at each iteration only s evaluations of a given multi-source activity index. The computational complexity of full-rank and reduced-rank indices is of the same order at each iteration. It shall be also emphasized that the above algorithm is just an example of an iterative scheme for computation of multi-source indices. Indeed, another iterative scheme with slightly more computational steps needed at each iteration has been proposed in [13].

B. Numerical Simulations

The simulations presented in this section use open-source EEG/MEG spatial filtering framework available for download at <https://github.com/IS-UMK/supFunSim.git>. It has been also used to generate numerical simulations in [24, Section VI]. We

describe below the key properties of this framework relevant to simulations considered in this paper.

Generation of time series in source space for bioelectrical activity of brains' cortical and subcortical regions is conducted using separate MVAR models (of order 6) for the active sources \mathbf{q}_0 and the biological background noise. We also add Gaussian uncorrelated noise to the time series in sensor space to obtain noise vector \mathbf{n} measured at the sensors. Moreover, the coefficient matrix of MVAR model used to generate \mathbf{q}_0 was multiplied by a non-diagonal mask matrix yielding correlated activity among active sources.

For solution of the forward problem, FieldTrip (FT) toolbox [20] was used for generation of volume conduction model (VCM) and leadfields. For the results presented herein, we arbitrarily select:

- *HydroCel Geodesic Sensor Net* utilizing 128 channels as EEG cap layout.
- Regions of interest (ROIs) corresponding to specific cortex patches, and whose geometry is reconstructed and parcellated from the detailed cortical surface by means of the Brainstorm toolbox [35]. We selected ROIs by their anatomical description in Destrieux and Desikan-Killiany atlases [4], [6]. Surface parcellation was prepared using freely available FreeSurfer Software Suite [3] such that each ROI is comprised of a triangular mesh and fully characterized by its nodes, from which candidates for source position and orientation (orthogonal to the mesh) will be randomly drawn.
- Both thalami modeled jointly as a single triangulated mesh containing node candidates for a random selection of subcortical bioelectrical activity. Also here, the orientation of sources is chosen as orthogonal to the mesh surface.

We considered 9 active sources, such that 3 of them were in fixed and closely positioned locations, with the locations of the remaining 6 randomly assigned among ROIs nodes, ensuring even distribution of sources among ROIs. The signal-to-noise ratio (SNR) was defined as $SNR = \|\mathbf{H}_0 \mathbf{q}_0\| / \|\mathbf{n}\|$. For each of the SNR ratio considered, we conducted 10 simulation runs. In each run, locations of 6 out of 9 active sources were randomly chosen in accordance to the above mentioned scheme, and a new MVAR model was used to generate the source signals.

Each simulation run contained a realization of the MVAR process with 1000 samples, where:

- The first half (i.e., the first 500 samples) of each trial is interpreted as pre-task/stimulus activity and represents noise signal \mathbf{n} . The estimate of noise covariance matrix \mathbf{N} is obtained from this section of the signals as a finite sample estimate.
- The second half of each trial is comprised of both noise and activity of sources \mathbf{q}_0 . The estimate of signal covariance matrix \mathbf{R} is obtained from this second section of the signals as a finite sample estimate.

We selected for evaluation the following activity indices, all of which are based on the activity indices introduced in

Sections II and III, adjusted for use in the iterative computation scheme considered in this section:

- MAI activity index defined at l -th iteration as:

$$\text{MAI} = \text{tr}\{\mathbf{G}\mathbf{S}^{-1}\} - l, \quad 1 \leq l \leq l_0. \quad (39)$$

- MAI_{ext} activity index defined at l -th iteration as:

$$\text{MAI}_{\text{ext}} = \begin{cases} \sum_{i=1}^l \lambda_i(\mathbf{G}\mathbf{S}^{-1}) - l, & 1 \leq l \leq r, \\ \sum_{i=1}^r \lambda_i(\mathbf{G}\mathbf{S}^{-1}) - r, & r < l \leq l_0. \end{cases} \quad (40)$$

We note that $\text{MAI}_{\text{ext}} = \text{MAI}$ for $1 \leq l \leq r$.

- MAI_{RR-I} activity index defined at l -th iteration as:

$$\text{MAI}_{RR-I} = \begin{cases} \text{tr}\{\mathbf{G}'(\mathbf{S}')^{-1}\} - l, & 1 \leq l \leq r, \\ \text{tr}\{\mathbf{G}\mathbf{S}^{-1}\mathbf{P}_S^{(r)}\} - r, & r < l \leq l_0. \end{cases} \quad (41)$$

We note that $\text{MAI}_{RR-I} = \text{MAI}$ for $1 \leq l \leq r$.

- MPZ activity index defined at l -th iteration as:

$$\text{MPZ} = \text{tr}\{\mathbf{S}\mathbf{T}^{-1}\} - l, \quad 1 \leq l \leq l_0. \quad (42)$$

- MPZ_{ext} activity index defined at l -th iteration as:

$$\text{MPZ}_{\text{ext}} = \begin{cases} \sum_{i=1}^l \lambda_i(\mathbf{S}\mathbf{T}^{-1}) - l, & 1 \leq l \leq r, \\ \sum_{i=1}^r \lambda_i(\mathbf{S}\mathbf{T}^{-1}) - r, & r < l \leq l_0. \end{cases} \quad (43)$$

We note that $\text{MPZ}_{\text{ext}} = \text{MPZ}$ for $1 \leq l \leq r$.

- MPZ_{RR-I} activity index defined at l -th iteration as:

$$\text{MPZ}_{RR-I} = \begin{cases} \text{tr}\{\mathbf{S}'(\mathbf{T}')^{-1}\} - l, & 1 \leq l \leq r, \\ \text{tr}\{\mathbf{S}\mathbf{T}^{-1}\mathbf{P}_S^{(r)}\} - r, & r < l \leq l_0. \end{cases} \quad (44)$$

We note that $\text{MPZ}_{RR-I} = \text{MPZ}$ for $1 \leq l \leq r$.

In the above formulation, only MAI and MPZ activity indices are unbiased in the sense of Definition 1. The reduced-rank activity indices MAI_{ext} and MPZ_{ext} are biased, while MAI_{RR-I} and MPZ_{RR-I} are unbiased under simplifying assumption of uncorrelated sources. Then, the analysis of key properties of MAI_{RR} and MPZ_{RR} activity indices made in Section III-B may be adjusted to current iterative scheme under this assumption. In particular, we selected their rank r used in Algorithm 1 as follows:⁵ first, we estimated the eigenvalues of $\lambda_i(\mathbf{G}'_0)$ for $1 \leq i \leq l_0$ from the l_0 largest eigenvalues of $\mathbf{R}\mathbf{N}^{-1}$, cf. (35). We then considered normalized eigen-

values as $\lambda'_i(\mathbf{R}\mathbf{N}^{-1}) := \lambda_i(\mathbf{R}\mathbf{N}^{-1}) / \sum_{i=1}^{l_0} \lambda_i(\mathbf{R}\mathbf{N}^{-1})$ for $1 \leq i \leq l_0$, and selected r such that

$$r = \arg \min_{1 \leq l \leq l_0} \sum_{i=1}^l \lambda'_i(\mathbf{R}\mathbf{N}^{-1}) > \delta \in (0, 1]. \quad (45)$$

The closer the δ is to 1, the less likely it becomes to discard trailing eigenvalues of $\mathbf{R}\mathbf{N}^{-1}$ (and hence, of $\lambda_i(\mathbf{G}'_0)$), thus reducing the possibility of obtaining reduced-rank activity index with increased spatial resolution compared with full-rank activity index, as discussed below Proposition 2 in Section III. On the other hand, if one chooses too small value of δ , from the same discussion it is seen that in such a case there is no guarantee that the resulting activity index will have better spatial resolution compared with full-rank activity index. In the current simulations, we set $\delta = 0.8$ to accommodate the above considerations.

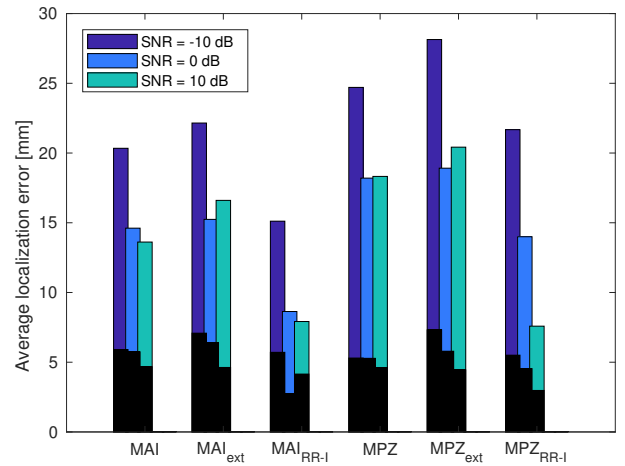


Fig. 2: Localization error averaged over simulation runs and all iterations of Algorithm 1. Black bars indicate standard deviations of corresponding localization errors.

TABLE I: Corresponding p -value of right-tailed Mann-Whitney-Wilcoxon test

SNR [dB]	hypothesis tested	
	$\text{MAI} > \text{MAI}_{RR-I}$	$\text{MAI}_{\text{ext}} > \text{MAI}_{RR-I}$
-10	0.0188	0.0086
0	0.0046	0.0057
10	0.007	0.0007
SNR [dB]	hypothesis tested	
	$\text{MPZ} > \text{MPZ}_{RR-I}$	$\text{MPZ}_{\text{ext}} > \text{MPZ}_{RR-I}$
-10	0.1061	0.032
0	0.0606	0.0378
10	0.0002	0.0002

At each iteration l of Algorithm 1, we measured the localization error defined as the Chebyshev distance between the source found by a given activity index and the closest active source. Figures 2 and 3 report averaged localization errors made by activity indices considered along with corresponding p -values of one-sided Mann-Whitney-Wilcoxon median test. It is seen that, in practice, SNR does matter, as the quality of estimates of \mathbf{R} and \mathbf{N} affects spatial resolution of indices and has an impact on the iterative implementation, cf. also [17].

⁵We used the same rank for MAI_{ext} and MPZ_{ext} activity indices as well.

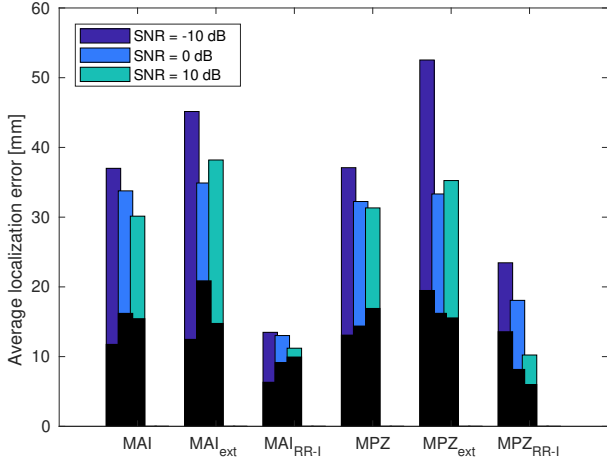


Fig. 3: Localization error averaged over simulation runs and sources found at last 2 iterations ($l \in \{l_0 - 1, l_0\}$) of Algorithm 1. Black bars indicate standard deviations of corresponding localization errors.

TABLE II: Corresponding p -value of right-tailed Mann-Whitney-Wilcoxon test

SNR [dB]	hypothesis tested	
	$MAI > MAI_{RR-I}$	$MAI_{ext} > MAI_{RR-I}$
-10	0.0003	0.0001
0	0.0007	0.0046
10	0.0023	0.0005
SNR [dB]	hypothesis tested	
	$MPZ > MPZ_{RR-I}$	$MPZ_{ext} > MPZ_{RR-I}$
-10	0.027	0.0018
0	0.0086	0.0086
10	0.0036	0.0007

The ranks selected for reduced-rank activity indices are shown on Figure 4. It is seen that they are stable across simulation runs, and that lower ranks are actually selected for higher SNR of 10 dB. In particular, as the maximal rank selected according to criterion in (45) for $\delta = 0.8$ was 7 across all SNR and all simulation runs, we presented in Figure 3 the

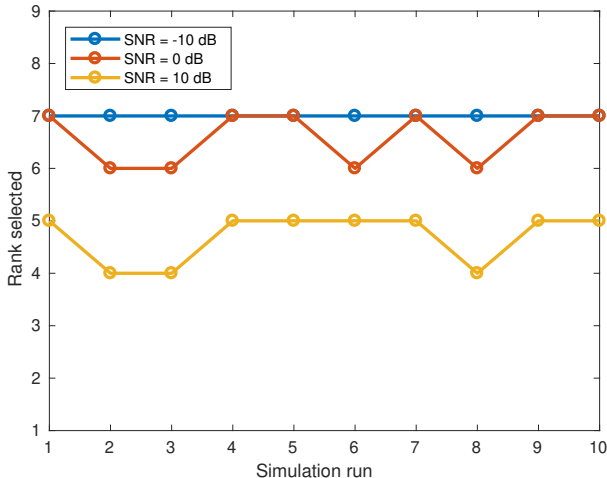


Fig. 4: Ranks selected across simulation runs according to criterion in (45) for $\delta = 0.8$.

averaged localization errors for the last 2 iterations of the algorithm, i.e., when the reduced-rank approach was always active. The gain in localization error is significant in this case, especially considering that the scale on y -axis representing average localization error in [mm] is doubled in Figure 3 compared with Figure 2.

V. CONCLUSIONS AND FUTURE WORK

We have introduced two novel families of reduced-rank activity indices and proved that they are unbiased for all nonzero rank constraints. We have also discussed conditions in which reducing the rank of activity index results in increased spatial resolution compared with its full-rank version. We presented a practical way to estimate rank of the reduced-rank activity index, and used it in a computationally efficient iterative scheme for discovering the sources. An alternative approach would be to develop a non-iterative optimization method capable of maximizing proposed multi-source activity indices directly in the l_0 -dimensional domain, which would allow their unbiased property to be used to maximum effect. Indeed, other activity indices, which are not amenable to iterative computations, such as the simple and appealing activity index $tr\{P_{\mathcal{R}(\mathbf{H})}(\mathbf{R} - \mathbf{N})\}$ (which uses the fact that $\mathbf{R} - \mathbf{N} = \mathbf{H}_0 \mathbf{C} \mathbf{H}_0^t$, and both \mathbf{R} and \mathbf{N} are estimable) could be investigated in such global optimization framework.

APPENDIX A OPTIMIZATION PROBLEMS LEADING TO LCMV AND MV-PURE FILTERS

The LCMV filter $\mathbf{W} \in \mathbb{R}^{l \times m}$ is the solution of the following optimization problem [7], [31], [37] with respect to \mathbf{X} :

$$\begin{cases} \text{minimize} & tr\{\mathbf{X}\mathbf{R}\mathbf{X}^t\} \\ \text{subject to} & \mathbf{X}\mathbf{H} = \mathbf{I}_l, \end{cases} \quad (46)$$

where $\mathbf{H} \in \mathbb{R}^{m \times l}$ is the leadfield matrix.⁶ We call the second condition in (46) *the unit-gain condition*. The solution to (46) is given in (4).

Furthermore, for a given rank constraint r such that $1 \leq r \leq l$, the MV-PURE filter $\mathbf{W}_r \in \mathbb{R}^{l \times m}$ is the solution of the following problem with respect to \mathbf{X} :

$$\begin{cases} \text{minimize} & tr\{\mathbf{X}\mathbf{R}\mathbf{X}^t\} \\ \text{subject to} & \mathbf{X} \in \bigcap_{\iota \in \mathcal{J}} \mathcal{P}_r^\iota, \end{cases} \quad (47)$$

with

$$\mathcal{P}_r^\iota = \underset{\mathbf{X} \in \mathcal{X}_r^{l \times m}}{\operatorname{argmin}} \|\mathbf{X}\mathbf{H} - \mathbf{I}_l\|_\iota^2, \iota \in \mathcal{J},$$

and

$$\mathcal{X}_r^{l \times m} = \{\mathbf{X} \in \mathbb{R}^{l \times m} : rank(\mathbf{X}) \leq r \leq l\},$$

where \mathcal{J} is the index set of all unitarily invariant norms, i.e., norms satisfying $\|\mathbf{U}\mathbf{X}\mathbf{V}\|_\iota = \|\mathbf{X}\|_\iota$ for all orthogonal $\mathbf{U} \in$

⁶Depending on the field of application, \mathbf{H} may be also called model or array response matrix.

$\mathbb{R}^{l \times l}$, $\mathbf{V} \in \mathbb{R}^{m \times m}$, and all $\mathbf{X} \in \mathbb{R}^{l \times m}$. The solution to (47) is given in [25] in the form (20).⁷

Remark 2. Comparison of optimization problems (46) and (47) reveals that the latter is essentially a reduced-rank extension of the former, with (46) being a special case of (47) for $r = l$. This fact justifies calling MV-PURE filter a natural reduced-rank extension of the LCMV filter, with MV-PURE yielding minimal deviation from unit-gain constraint $\mathbf{X}\mathbf{H} = \mathbf{I}_l$ among filters of rank r .

APPENDIX B

SPATIAL RESOLUTION OF MAI AND MPZ ACTIVITY INDICES

Fact 1 ([17]). *MPZ has higher spatial resolution than MAI.*

Sketch of proof: The proof of the fact that MPZ has higher spatial resolution than MAI (cf. Definition 2) has been obtained in [17] based on inequality derived in [17, Appendix A]:

$$\mathbf{T} \succeq \mathbf{S}(\mathbf{G})^{-1}\mathbf{S}, \quad (48)$$

for \mathbf{S} , \mathbf{G} , and \mathbf{T} defined in (5), (8) and (12), respectively, with equality achieved at $\boldsymbol{\theta}_0$. Namely, from (48) one has that

$$\mathbf{T}^{-1} \preceq (\mathbf{S}(\mathbf{G})^{-1}\mathbf{S})^{-1} = \mathbf{S}^{-1}\mathbf{G}\mathbf{S}^{-1}.$$

Then, from the definitions of MAI and MPZ activity indices in (14) and (15), respectively, we obtain

$$\begin{aligned} MPZ(\boldsymbol{\theta}) &= \text{tr}\{\mathbf{S}\mathbf{T}^{-1}\} - l = \text{tr}\{\mathbf{S}^{1/2}\mathbf{T}^{-1}\mathbf{S}^{1/2}\} - l \leq \\ &\text{tr}\{\mathbf{S}^{1/2}\mathbf{S}^{-1}\mathbf{G}\mathbf{S}^{-1}\mathbf{S}^{1/2}\} - l = \text{tr}\{\mathbf{G}\mathbf{S}^{-1}\} - l = MAI(\boldsymbol{\theta}), \end{aligned}$$

satisfying the first condition in (3). The equality $\mathbf{T}(\boldsymbol{\theta}_0) = \mathbf{S}(\boldsymbol{\theta}_0)\mathbf{G}(\boldsymbol{\theta}_0)^{-1}\mathbf{S}(\boldsymbol{\theta}_0)$ ensures the second condition in (3), completing the proof. ■

APPENDIX C

PROOF OF LEMMA 1

Let $\mathbf{U}\boldsymbol{\Sigma}\mathbf{V}^t$ be the singular value decomposition of $\mathbf{R}^{-1/2}\mathbf{H}'$ with diagonal entries of $\boldsymbol{\Sigma}$ organized in non-increasing order. Then $\mathbf{H}' = \mathbf{R}^{1/2}\mathbf{U}\boldsymbol{\Sigma}\mathbf{V}^t$ and hence

$$\begin{aligned} MAI_{RR}(\boldsymbol{\theta}, r) + r &= \text{tr}\{\mathbf{V}\boldsymbol{\Sigma}^t\mathbf{U}^t\mathbf{R}^{1/2}\mathbf{N}^{-1}\mathbf{R}^{1/2}\mathbf{U}\boldsymbol{\Sigma}\mathbf{V}^t \\ &\quad (\mathbf{V}\boldsymbol{\Sigma}^t\mathbf{U}^t\mathbf{U}\boldsymbol{\Sigma}\mathbf{V}^t)^{-1}\mathbf{V}\mathbf{I}_l^r\mathbf{V}^t\} = \\ &\text{tr}\{\boldsymbol{\Sigma}^t\mathbf{U}^t\mathbf{R}^{1/2}\mathbf{N}^{-1}\mathbf{R}^{1/2}\mathbf{U}\boldsymbol{\Sigma}(\boldsymbol{\Sigma}^t\boldsymbol{\Sigma})^{-1}\mathbf{I}_l^r\} = \\ &\text{tr}\{\mathbf{R}^{1/2}\mathbf{N}^{-1}\mathbf{R}^{1/2}\mathbf{U}\boldsymbol{\Sigma}(\boldsymbol{\Sigma}^t\boldsymbol{\Sigma})^{-1}\mathbf{I}_l^r\boldsymbol{\Sigma}^t\mathbf{U}^t\} = \\ &\text{tr}\{\mathbf{R}^{1/2}\mathbf{N}^{-1}\mathbf{R}^{1/2}\mathbf{U}\mathbf{I}_m^r\mathbf{U}^t\} \leq \sum_{i=1}^r \lambda_i(\mathbf{R}^{1/2}\mathbf{N}^{-1}\mathbf{R}^{1/2}) \\ &= \sum_{i=1}^r \lambda_i(\mathbf{R}\mathbf{N}^{-1}). \quad (49) \end{aligned}$$

⁷The work [25] considers a more general problem where additional linear constraints are imposed on the resulting estimator/filter. The optimization problem (47) and the resulting solution (20) are considered in [25] for the case of no linear constraints.

The essential inequality above is obtained from Theobald's theorem (Fact 2 in Appendix G). This proves the first inequality in (27). Then, to complete the proof of (27) we note that $\mathbf{R} = \mathbf{H}'_0(\mathbf{H}'_0)^t + \mathbf{N}$, so using (49) we obtain

$$\begin{aligned} MAI_{RR}(\boldsymbol{\theta}, r) &\leq \sum_{i=1}^r \lambda_i(\mathbf{R}\mathbf{N}^{-1}) - r = \\ &\sum_{i=1}^r \lambda_i(\mathbf{H}'_0(\mathbf{H}'_0)^t\mathbf{N}^{-1} + \mathbf{I}_m) - r = \sum_{i=1}^r \lambda_i(\mathbf{G}'_0). \quad \blacksquare \quad (50) \end{aligned}$$

APPENDIX D

PROOF OF THEOREM 1

a) *MAI_{RR} is unbiased:* Remark 3 below Fact 3 in Appendix G states that

$$(\mathbf{S}'_0)^{-1} = (\mathbf{G}'_0)^{-1} + \mathbf{I}_{l_0}, \quad (51)$$

and hence in particular

$$\mathbf{P}_{\mathbf{S}'_0}^{(r)} = \mathbf{P}_{\mathbf{G}'_0}^{(r)}. \quad (52)$$

Then, by (51) and (52)

$$\begin{aligned} MAI_{RR}(\boldsymbol{\theta}_0, r) &= \text{tr}\{\mathbf{G}'_0(\mathbf{S}'_0)^{-1}\mathbf{P}_{\mathbf{S}'_0}^{(r)}\} - r = \\ &\text{tr}\{(\mathbf{I}_{l_0} + \mathbf{G}'_0)\mathbf{P}_{\mathbf{G}'_0}^{(r)}\} - r = \text{tr}\{\mathbf{G}'_0\mathbf{P}_{\mathbf{G}'_0}^{(r)}\} = \sum_{i=1}^r \lambda_i(\mathbf{G}'_0), \quad (53) \end{aligned}$$

establishing unbiasedness of *MAI_{RR}* in view of (27).

b) *MPZ_{RR} is unbiased and has higher spatial resolution than MAI_{RR}:* From (48) in Appendix B we obtain

$$\mathbf{T}' \succeq \mathbf{S}'(\mathbf{G}')^{-1}\mathbf{S}',$$

hence

$$(\mathbf{S}')^{-1}\mathbf{G}'(\mathbf{S}')^{-1} \succeq (\mathbf{T}')^{-1}, \quad (54)$$

with equality achieved at $\boldsymbol{\theta}_0$. Consequently,

$$\begin{aligned} \sum_{i=1}^r \lambda_i(\mathbf{G}'_0) &= MAI_{RR}(\boldsymbol{\theta}_0, r) = \text{tr}\{\mathbf{S}'_0(\mathbf{T}'_0)^{-1}\mathbf{P}_{\mathbf{S}'_0}^{(r)}\} - r = \\ &\text{tr}\{\mathbf{S}'_0((\mathbf{S}'_0)^{-1}\mathbf{G}'_0(\mathbf{S}'_0)^{-1})\mathbf{P}_{\mathbf{S}'_0}^{(r)}\} - r = MPZ_{RR}(\boldsymbol{\theta}_0, r). \quad (55) \end{aligned}$$

Let now $\mathbf{V}\boldsymbol{\Lambda}\mathbf{V}^t$ be the eigenvalue decomposition of \mathbf{S}' with eigenvalues organized in non-increasing order. Then, using similar algebraic manipulations as in (23) and the fact that $(\mathbf{S}')^{1/2} = \mathbf{V}\boldsymbol{\Lambda}^{1/2}\mathbf{V}^t$ we obtain

$$\mathbf{P}_{\mathbf{S}'}^{(r)}\mathbf{S}' = \mathbf{V}\mathbf{I}_l^r\boldsymbol{\Lambda}\mathbf{V}^t = (\mathbf{S}')^{1/2}\mathbf{P}_{\mathbf{S}'}^{(r)}\mathbf{P}_{\mathbf{S}'}^{(r)}(\mathbf{S}')^{1/2},$$

and

$$(\mathbf{S}')^{-1}\mathbf{P}_{\mathbf{S}'}^{(r)} = \mathbf{V}\boldsymbol{\Lambda}^{-1}\mathbf{I}_l^r\mathbf{V}^t = (\mathbf{S}')^{-1/2}\mathbf{P}_{\mathbf{S}'}^{(r)}\mathbf{P}_{\mathbf{S}'}^{(r)}(\mathbf{S}')^{-1/2}.$$

Therefore, using (54) one has that

$$\begin{aligned} MPZ_{RR}(\boldsymbol{\theta}, r) + r &= \text{tr}\{\mathbf{S}'(\mathbf{T}')^{-1}\mathbf{P}_{\mathbf{S}'}^{(r)}\} = \\ &\text{tr}\{\mathbf{P}_{\mathbf{S}'}^{(r)}(\mathbf{S}')^{1/2}(\mathbf{T}')^{-1}(\mathbf{S}')^{1/2}\mathbf{P}_{\mathbf{S}'}^{(r)}\} \leq \\ &\text{tr}\{\mathbf{P}_{\mathbf{S}'}^{(r)}(\mathbf{S}')^{1/2}(\mathbf{S}')^{-1}\mathbf{G}'(\mathbf{S}')^{-1}(\mathbf{S}')^{1/2}\mathbf{P}_{\mathbf{S}'}^{(r)}\} = \end{aligned}$$

$$\begin{aligned} \text{tr}\{\mathbf{G}'(\mathbf{S}')^{-1/2}\mathbf{P}_{\mathbf{S}'}^{(r)}\mathbf{P}_{\mathbf{S}'}^{(r)}(\mathbf{S}')^{-1/2}\} &= \text{tr}\{\mathbf{G}'(\mathbf{S}')^{-1}\mathbf{P}_{\mathbf{S}'}^{(r)}\} = \\ &= \text{MAI}_{RR}(\boldsymbol{\theta}, r) + r, \end{aligned}$$

and thus $\text{MPZ}_{RR}(\boldsymbol{\theta}, r) \leq \text{MAI}_{RR}(\boldsymbol{\theta}, r)$. In view of unbiasedness of MAI_{RR} and (55) this completes the proof. ■

APPENDIX E PROOF OF PROPOSITION 2

By applying matrix inversion lemma [14] to

$$\mathbf{R} = \mathbf{H}_0\mathbf{Q}\mathbf{H}_0^t + \mathbf{N} = \mathbf{H}_0'(\mathbf{H}_0')^t + \mathbf{N}$$

one has

$$\mathbf{R}^{-1} = \mathbf{N}^{-1} - \mathbf{N}^{-1}\mathbf{H}_0'(\mathbf{I}_{l_0} + (\mathbf{H}_0')^t\mathbf{N}^{-1}\mathbf{H}_0')^{-1}(\mathbf{H}_0')^t\mathbf{N}^{-1}. \quad (56)$$

We obtain thus that $\mathbf{G}' = \mathbf{S}' + \mathbf{Y}_1$, where $\mathbf{Y}_1 = \mathbf{K}'\mathbf{Z}(\mathbf{K}')^t$ with $\mathbf{Z} = (\mathbf{I}_{l_0} + \mathbf{G}_0')^{-1} \succ 0$ and $\mathbf{K}' = (\mathbf{H}')^t\mathbf{N}^{-1}\mathbf{H}_0'$. Note that the matrix \mathbf{Y}_1 is positive semidefinite, $\mathbf{Y}_1 \succeq 0$, and let r_1 and r_2 be such that $1 \leq r_1 \leq r_2 \leq l_0$. Denote $\mathbf{Y}_p = \mathbf{P}_{\mathbf{S}'}^{(r_2)} - \mathbf{P}_{\mathbf{S}'}^{(r_1)} \succeq 0$. Then, using similar algebraic manipulations as in (23) it is seen that

$$\mathbf{Y}_p(\mathbf{S}')^{-1}\mathbf{Y}_p = (\mathbf{S}')^{-1}\mathbf{Y}_p \succeq 0 \quad \text{and} \quad \mathbf{Y}_p\mathbf{S}'\mathbf{Y}_p = \mathbf{Y}_p\mathbf{S}' \succeq 0. \quad (57)$$

Therefore,

$$\begin{aligned} \text{MAI}_{RR}(\boldsymbol{\theta}, r_2) - \text{MAI}_{RR}(\boldsymbol{\theta}, r_1) &= \\ \text{tr}\{\mathbf{G}'(\mathbf{S}')^{-1}[\mathbf{P}_{\mathbf{S}'}^{(r_2)} - \mathbf{P}_{\mathbf{S}'}^{(r_1)}]\} - (r_2 - r_1) &= \\ \text{tr}\{(\mathbf{S}' + \mathbf{Y}_1)(\mathbf{S}')^{-1}\mathbf{Y}_p\} - (r_2 - r_1) &= \\ \text{tr}\{\mathbf{Y}_1(\mathbf{S}')^{-1}\mathbf{Y}_p\} = \text{tr}\{\mathbf{Y}_1^{1/2}(\mathbf{S}')^{-1}\mathbf{Y}_p\mathbf{Y}_1^{1/2}\} &\geq 0, \end{aligned}$$

as $\mathbf{Y}_1^{1/2}(\mathbf{S}')^{-1}\mathbf{Y}_p\mathbf{Y}_1^{1/2} \succeq 0$. Using now expression of \mathbf{R}^{-1} as in (56), we obtain that $\mathbf{T}' = (\mathbf{H}')^t\mathbf{R}^{-1}\mathbf{N}\mathbf{R}^{-1}\mathbf{H}'$ satisfies (cf. [17, Appendix A])

$$\mathbf{T}' = \mathbf{S}' - [\mathbf{K}'\mathbf{Z}(\mathbf{K}')^t - \mathbf{K}'\mathbf{Z}\mathbf{G}_0'\mathbf{Z}(\mathbf{K}')^t]. \quad (58)$$

Note that $\mathbf{Z}^{-1} = \mathbf{I}_{l_0} + \mathbf{G}_0' \succ \mathbf{G}_0'$, hence $\mathbf{Z} \succ \mathbf{Z}\mathbf{G}_0'\mathbf{Z}$, and consequently $\mathbf{K}'\mathbf{Z}(\mathbf{K}')^t \succeq \mathbf{K}'\mathbf{Z}\mathbf{G}_0'\mathbf{Z}(\mathbf{K}')^t$. From (58) we obtain therefore that $\mathbf{T}' = \mathbf{S}' - \mathbf{Y}_2$, where \mathbf{Y}_2 is positive semidefinite, i.e., $\mathbf{T}' \preceq \mathbf{S}'$, and hence

$$(\mathbf{T}')^{-1} \succeq (\mathbf{S}')^{-1}. \quad (59)$$

By definition, there exists $\mathbf{Y}_3 \succeq 0$ such that $(\mathbf{T}')^{-1} = (\mathbf{S}')^{-1} + \mathbf{Y}_3$. Using this fact, from (57), and proceeding similarly as above for MAI_{RR} we obtain that

$$\begin{aligned} \text{MPZ}_{RR}(\boldsymbol{\theta}, r_2) - \text{MPZ}_{RR}(\boldsymbol{\theta}, r_1) &= \\ \text{tr}\{\mathbf{S}'(\mathbf{T}')^{-1}[\mathbf{P}_{\mathbf{S}'}^{(r_2)} - \mathbf{P}_{\mathbf{S}'}^{(r_1)}]\} - (r_2 - r_1) &= \\ \text{tr}\{\mathbf{S}'[(\mathbf{S}')^{-1} + \mathbf{Y}_3]\mathbf{Y}_p\} - (r_2 - r_1) &= \\ \text{tr}\{\mathbf{Y}_p\mathbf{S}'\mathbf{Y}_3\} = \text{tr}\{\mathbf{Y}_3^{1/2}\mathbf{Y}_p\mathbf{S}'\mathbf{Y}_3^{1/2}\} &\geq 0, \end{aligned}$$

as $\mathbf{Y}_3^{1/2}\mathbf{Y}_p\mathbf{S}'\mathbf{Y}_3^{1/2} \succeq 0$. This completes the proof. ■

APPENDIX F PROOF OF PROPOSITION 3

For $i \in \{1, \dots, l\}$ one has

$$\begin{aligned} \lambda_i(\mathbf{G}\mathbf{S}^{-1}) &= \lambda_i(\mathbf{G}'(\mathbf{S}')^{-1}) = \\ &= \lambda_i((\mathbf{G}')^{1/2}(\mathbf{S}')^{-1}(\mathbf{G}')^{1/2}) \geq \\ &= \lambda_i((\mathbf{G}')^{1/2}(\mathbf{S}')^{-1}\mathbf{P}_{\mathbf{S}'}^{(r)}(\mathbf{G}')^{1/2}) = \lambda_i(\mathbf{G}'(\mathbf{S}')^{-1}\mathbf{P}_{\mathbf{S}'}^{(r)}), \end{aligned}$$

where the inequality follows from [14, Corollary 7.7.4], as $(\mathbf{S}')^{-1} \succeq (\mathbf{S}')^{-1}\mathbf{P}_{\mathbf{S}'}^{(r)}$, cf. also (23). This proves (36), as $\sum_{i=1}^r \lambda_i(\mathbf{G}'(\mathbf{S}')^{-1}\mathbf{P}_{\mathbf{S}'}^{(r)}) = \text{tr}\{\mathbf{G}'(\mathbf{S}')^{-1}\mathbf{P}_{\mathbf{S}'}^{(r)}\}$. Moreover, from Fact 3 in Appendix G one has

$$\begin{aligned} \text{MAI}_{ext}(\boldsymbol{\theta}_0, r) &= \sum_{i=1}^r \lambda_i(\mathbf{G}_0\mathbf{S}_0^{-1}) - r = \sum_{i=1}^r \lambda_i(\mathbf{G}_0\mathbf{Q}) = \\ &= \sum_{i=1}^r \lambda_i(\mathbf{G}_0') = \text{MAI}_{RR}(\boldsymbol{\theta}_0, r). \quad (60) \end{aligned}$$

The proof of (37) follows similarly as above:

$$\begin{aligned} \lambda_i(\mathbf{S}\mathbf{T}^{-1}) &= \lambda_i(\mathbf{S}'(\mathbf{T}')^{-1}) = \\ &= \lambda_i((\mathbf{T}')^{-1/2}\mathbf{S}'(\mathbf{T}')^{-1/2}) \geq \\ &= \lambda_i((\mathbf{T}')^{-1/2}\mathbf{P}_{\mathbf{S}'}^{(r)}\mathbf{S}'(\mathbf{T}')^{-1/2}) = \lambda_i(\mathbf{S}'(\mathbf{T}')^{-1}\mathbf{P}_{\mathbf{S}'}^{(r)}), \end{aligned}$$

where the inequality follows from [14, Corollary 7.7.4], as in this case $\mathbf{S}' \succeq \mathbf{P}_{\mathbf{S}'}^{(r)}\mathbf{S}'$. This proves (37), as $\sum_{i=1}^r \lambda_i(\mathbf{S}'(\mathbf{T}')^{-1}\mathbf{P}_{\mathbf{S}'}^{(r)}) = \text{tr}\{\mathbf{S}'(\mathbf{T}')^{-1}\mathbf{P}_{\mathbf{S}'}^{(r)}\}$. We recall now from Fact 1 in Appendix B that equality is achieved in (48) for $\boldsymbol{\theta}_0$, i.e., $\mathbf{T}_0 = \mathbf{S}_0\mathbf{G}_0^{-1}\mathbf{S}_0$, and hence $\mathbf{T}_0^{-1} = \mathbf{S}_0^{-1}\mathbf{G}_0\mathbf{S}_0^{-1}$. Thus,

$$\text{MPZ}_{ext}(\boldsymbol{\theta}_0, r) = \sum_{i=1}^r \lambda_i(\mathbf{S}_0\mathbf{T}_0^{-1}) - r = \sum_{i=1}^r \lambda_i(\mathbf{G}_0\mathbf{S}_0^{-1}) - r.$$

In view of (60) and (28) in Theorem 1 this completes the proof of (38). ■

APPENDIX G KNOWN RESULTS USED

Fact 2 ([36]). *Let $\mathbf{C} \in \mathbb{R}^{n \times n}$, $\mathbf{D} \in \mathbb{R}^{n \times n}$ be symmetric matrices. Denoting by $c_1 \geq c_2 \geq \dots \geq c_n$ and $d_1 \geq d_2 \geq \dots \geq d_n$ the eigenvalues of \mathbf{C} and \mathbf{D} , respectively, one has*

$$\text{tr}\{\mathbf{C}\mathbf{D}\} \leq \sum_{i=1}^n c_i d_i. \quad (61)$$

*The equality can be attained.*⁸

The following Fact 3 is well-known and can be obtained, e.g., by applying matrix inversion lemma [14] to \mathbf{S}_0 . It is stated explicitly in [26].

Fact 3 ([26]). *With notation as in model (1), one has*

$$\mathbf{S}_0^{-1} = \mathbf{G}_0^{-1} + \mathbf{Q}. \quad (62)$$

Remark 3. *In terms of model (18), from (62) we obtain in this case*

$$(\mathbf{S}'_0)^{-1} = (\mathbf{G}'_0)^{-1} + \mathbf{I}_{l_0}. \quad (63)$$

⁸The work [36] gives explicit form of eigenvalue decompositions of \mathbf{C} and \mathbf{D} for which equality can be attained.

Fact 4 (Lidskii’s Theorem, p. 248 [16]). *If $\mathbf{G}, \mathbf{H} \in \mathbb{C}^{n \times n}$ are positive semidefinite Hermitian, and $1 \leq i_1 < \dots < i_k \leq n$, then*

$$\prod_{t=1}^k \lambda_{i_t}(\mathbf{GH}) \leq \prod_{t=1}^k \lambda_{i_t}(\mathbf{G})\lambda_{i_t}(\mathbf{H}). \quad (64)$$

ACKNOWLEDGMENT

The authors would like to thank Mr. Mateusz Wilk for his help with simplifying the proof of Lemma 1 and conducting simulations. The authors would also like to thank Dr. Joanna Dreszer for her continuous support and encouragement.

REFERENCES

- [1] S. Baillet, J. C. Mosher, and R. M. Leahy. Electromagnetic brain mapping. *IEEE Signal Process. Mag.*, 18(6):14–30, 2001.
- [2] S. S. Dalal, K. Sekihara, and S. S. Nagarajan. Modified beamformers for coherent source region suppression. *IEEE Trans. Biomed. Eng.*, 53(7):1357–1363, July 2006.
- [3] Anders M. Dale, Bruce Fischl, and Martin I. Sereno. Cortical surface-based analysis: I. segmentation and surface reconstruction. *NeuroImage*, 9(2):179–194, 1999.
- [4] Rahul S. Desikan, Florent Sgonne, Bruce Fischl, Brian T. Quinn, Bradford C. Dickerson, Deborah Blacker, Randy L. Buckner, Anders M. Dale, R. Paul Maguire, Bradley T. Hyman, Marilyn S. Albert, and Ronald J. Killiany. An automated labeling system for subdividing the human cerebral cortex on MRI scans into gyral based regions of interest. *NeuroImage*, 31(3):968–980, 2006.
- [5] M. Diwakar, M.-X. Huang, R. Srinivasan, D. L. Harrington, A. Robb, A. Angeles, L. Muzzatti, R. Pakdaman, T. Song, R. J. Theilmann, and R. R. Lee. Dual-core beamformer for obtaining highly correlated neuronal networks in MEG. *NeuroImage*, 54(1):253–263, January 2011.
- [6] Bruce Fischl, Andr van der Kouwe, Christophe Destrieux, Eric Halgren, Florent Sgonne, David H. Salat, Evelina Busa, Larry J. Seidman, Jill Goldstein, David Kennedy, Verne Caviness, Nikos Makris, Bruce Rosen, and Anders M. Dale. Automatically parcellating the human cerebral cortex. *Cerebral Cortex*, 14(1):11–22, 2004.
- [7] O. T. Frost. An algorithm for linearly constrained adaptive array processing. *Proc. IEEE*, 60(8):926–935, August 1972.
- [8] A. Gramfort, M. Luessi, E. Larson, D. Engemann, D. Strohmeier, C. Brodbeck, L. Parkkonen, and M. Hämäläinen. MNE software for processing MEG and EEG data. *NeuroImage*, 86:446–460, 2014.
- [9] R. E. Greenblatt, A. Ossadchi, and M. E. Pflieger. Local linear estimators for the bioelectromagnetic inverse problem. *IEEE Trans. Signal Process.*, 53(9):3403–3412, 2005.
- [10] J. Gross, J. Kujala, M. Hämäläinen, L. Timmermann, A. Schnitzler, and R. Salmelin. Dynamic imaging of coherent sources: Studying neural interactions in the human brain. *Proceedings of the National Academy of Sciences*, 98(2):694–699, 2001.
- [11] M. Hämäläinen, R. Hari, R. J. Ilmoniemi, J. Knuutila, and O. V. Lounasmaa. Magnetoencephalography-theory, instrumentation, and applications to noninvasive studies of the working human brain. *Rev. Mod. Phys.*, 65:413–497, Apr 1993.
- [12] H. Helmholtz. Ueber einige gesetze der vertheilung elektrischer ströme in körperlichen leitern, mit anwendung auf die thierisch-elektrischen versuche (schluss.). *Annalen der Physik*, 165(7):353–377, 1853.
- [13] A. T. Herdman, A. Moiseev, and U. Ribary. Localizing event-related potentials using multi-source minimum variance beamformers: A validation study. *Brain Topography*, 31(4):546–565, July 2018.
- [14] R. A. Horn and C. R. Johnson. *Matrix Analysis*. Cambridge University Press, New York, 1985.
- [15] A. Keitel and J. Gross. Individual human brain areas can be identified from their characteristic spectral activation fingerprints. *PLoS Biol.*, 14(6):e1002498, 2016.
- [16] A. W. Marshall and I. Olkin. *Inequalities: Theory of Majorization and Its Applications*. Academic, New York, 1979.
- [17] A. Moiseev, J. M. Gaspar, J. A. Schneider, and A. T. Herdman. Application of multi-source minimum variance beamformers for reconstruction of correlated neural activity. *NeuroImage*, 58(2):481–496, September 2011.
- [18] A. Moiseev and A. T. Herdman. Multi-core beamformers: Derivation, limitations and improvements. *NeuroImage*, 71:135 – 146, 2013.
- [19] J. C. Mosher, R. M. Leahy, and P. S. Lewis. EEG and MEG: forward solutions for inverse methods. *IEEE Trans. Biomed. Eng.*, 46(3):245–259, March 1999.
- [20] R. Oostenveld, P. Fries, E. Maris, and J.-M. Schoffelen. FieldTrip: Open source software for advanced analysis of MEG, EEG, and invasive electrophysiological data. *Computational Intelligence and Neuroscience*, (156869), 2011.
- [21] T. Piotrowski, R. L. G. Cavalcante, and I. Yamada. Stochastic MV-PURE estimator: Robust reduced-rank estimator for stochastic linear model. *IEEE Trans. Signal Process.*, 57(4):1293–1303, April 2009.
- [22] T. Piotrowski, D. Gutierrez, I. Yamada, and J. Zygierevicz. A family of reduced-rank neural activity indices for EEG/MEG source localization. *LNCSS*, 8609:447–458, August 2014.
- [23] T. Piotrowski, D. Gutierrez, I. Yamada, and J. Zygierevicz. Reduced-rank neural activity index for EEG/MEG multi-source localization. In *Proc. IEEE ICASSP*, pages 4708–4712, Florence, Italy, May 2014.
- [24] T. Piotrowski, J. Nikadon, and D. Gutiérrez. Reconstruction of brain activity from EEG/MEG using MV-PURE framework. *IEEE Trans. Signal Process.* (submitted).
- [25] T. Piotrowski and I. Yamada. MV-PURE estimator: Minimum-variance pseudo-unbiased reduced-rank estimator for linearly constrained ill-conditioned inverse problems. *IEEE Trans. Signal Process.*, 56(8):3408–3423, August 2008.
- [26] T. Piotrowski and I. Yamada. Performance of the stochastic MV-PURE estimator in highly noisy settings. *J. of the Franklin Institute*, 351(6):3339–3350, June 2014.
- [27] M. Popescu, E. A. Popescu, T. Chan, S. D. Blunt, and J. D. Lewine. Spatio-temporal reconstruction of bilateral auditory steady-state responses using MEG beamformers. *IEEE Trans. Biomed. Eng.*, 55(3):1092–1102, March 2008.
- [28] M. A. Quraan and D. Cheyne. Reconstruction of correlated brain activity with adaptive spatial filters in MEG. *NeuroImage*, 49(3):2387 – 2400, 2010.
- [29] S. Robinson and J. Vrba. Functional neuroimaging by synthetic aperture magnetometry (sam). In *Recent Advances in Biomagnetism*, pages 302–305, Sendai, Japan, September 1998.
- [30] L. L. Scharf. The SVD and reduced rank signal processing. *Signal Process.*, 25:113–133, 1991.
- [31] K. Sekihara and S. S. Nagarajan. *Adaptive Spatial Filters for Electromagnetic Brain Imaging*. Springer-Verlag, Berlin, 2008.
- [32] K. Sekihara, S. S. Nagarajan, D. Poeppel, A. Marantz, and Y. Miyashita. Reconstructing spatio-temporal activities of neural sources using an MEG vector beamformer technique. *IEEE Trans. Biomed. Eng.*, 48(7):760–771, July 2001.
- [33] M. Siems, A.-A. Pape, J. F. Hipp, and M. Siegel. Measuring the cortical correlation structure of spontaneous oscillatory activity with EEG and MEG. *NeuroImage*, 129:345–355, 2016.
- [34] P. Stoica and M. Viberg. Maximum likelihood parameter and rank estimation in reduced-rank multivariate linear regressions. *IEEE Trans. Signal Process.*, 44(12):3069–3078, December 1996.
- [35] F. Tadel, S. Baillet, J.C. Mosher, D. Pantazis, and R. M. Leahy. Brainstorm: A user-friendly application for MEG/EEG analysis. *Computational Intelligence and Neuroscience*, (879716), 2011.
- [36] C. M. Theobald. An inequality for the trace of the product of two symmetric matrices. *Math. Proc. Camb. Phil. Soc.*, 77:265–267, 1975.
- [37] B. D. Van Veen, W. Van Dronghen, M. Yuchtman, and A. Suzuki. Localization of brain electrical activity via linearly constrained minimum variance spatial filtering. *IEEE Trans. Biomed. Eng.*, 44(9):867–880, September 1997.
- [38] K. Werner and M. Jansson. Reduced rank linear regression and weighted low rank approximations. *IEEE Trans. Signal Process.*, 53(6):2063–2075, June 2006.
- [39] I. Yamada and J. Elbadraoui. Minimum-variance pseudo-unbiased low-rank estimator for ill-conditioned inverse problems. In *Proc. IEEE ICASSP*, pages 325–328, Toulouse, France, May 2006.